

Enhancing dissipative cat-state generation via nonequilibrium pump fields

Zheng-Yang Zhou,^{1,2} Clemens Gneiting,^{2,3} Wei Qin,² J. Q. You,^{4,1,*} and Franco Nori^{2,3,5,†}

¹*Beijing Computational Science Research Center, Beijing 100094, China*

²*Theoretical Quantum Physics Laboratory, RIKEN Cluster for Pioneering Research, Wako-shi, Saitama 351-0198, Japan*

³*RIKEN Center for Quantum Computing (RQC),*

²⁻¹*Hirosawa, Wako-shi, Saitama 351-0198, Japan*

⁴*Interdisciplinary Center of Quantum Information,*

State Key Laboratory of Modern Optical Instrumentation,

and Zhejiang Province Key Laboratory of Quantum Technology and Device,

Department of Physics, Zhejiang University, Hangzhou 310027, China

⁵*Physics Department, The University of Michigan, Ann Arbor, Michigan 48109-1040, USA*

(Dated: January 27, 2022)

Cat states, which were initially proposed to manifest macroscopic superpositions, play an outstanding role in fundamental aspects of quantum dynamics. In addition, they have potential applications in quantum computation and quantum sensing. However, cat states are vulnerable to dissipation, which puts the focus of cat-state generation on higher speed and increased robustness. Dissipative cat-state generation is a common approach based on the nonlinear coupling between a lossy pump field and a half-frequency signal field. In such an approach, the pump field is usually kept in equilibrium, which limits the cat-state generation. We show that the equilibrium requirement can be removed by introducing a synchronous pump method. In this nonequilibrium regime, the speed of the cat-state generation can be increased by one order of magnitude, and the robustness to single-photon loss can be enhanced. The realization of synchronous pumps is discussed for both time-multiplexed systems and standing modes.

Introduction.—Optical cat states stem from the concept of “Schrödinger’s cat”, which is almost synonymous with quantum mechanics. Therefore, generating such states in different systems is of fundamental relevance [1–7]. In addition, cat states have practical applications in fields of quantum metrology [8–12] and quantum computation [13–18]. A common method to generate cat states relies on dissipation, where cat states emerge as a result of the competition between the two-photon pumping and the two-photon loss [5, 19–23]. Typically, nonlinear couplings are weak compared to the linear ones. Two-photon effects in dissipative cat-state generation are even weaker because these effects are induced by a nonlinear coupling to an adiabatic pump field. Therefore, cat states are sensitive to single-photon loss, so the generation and storage of such states are challenging [24–27]. Larger nonlinearities are most obvious solutions but require significant improvements in experimental technologies. An alternative way is to achieve stronger two-photon processes with currently accessible nonlinearities.

The pump fields and the signal fields can be conceived as either standing modes (zero group velocity) [28, 29] or traveling modes (nonzero group velocity) [30–36] as illustrated in Fig. 1. Standing modes are usually eigenmodes of the systems, while traveling modes correspond to pulses which are typically superpositions of different eigenmodes in a cyclic arrangement. As different traveling modes pass the pump devices periodically at different times, synchronous pumping is used to control the pump-

ing intensities on these modes. Although both standing modes and traveling modes can be described using the same theory in most cases [37, 38], traveling modes can exhibit unique properties, such as the decoupling of the pump modes and the signal modes due to group-velocity difference or crystal length [34, 35]. An important application of traveling modes and synchronous pumping is the coherent Ising machine [6, 39–42], which can simulate large spin systems. As cat states are potential quantum outputs in the coherent Ising machine, their generation is significant for such traveling mode arrangements. Therefore, it is natural to ask whether cat-state generation can benefit from the special properties of synchronous pumping.

To answer these questions, we analyze cat-state generation based on the synchronous pumping. In our

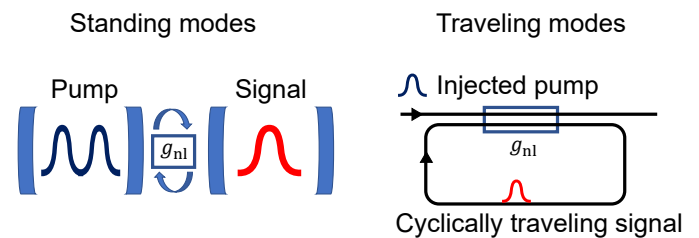


FIG. 1. Illustrations of standing-mode and traveling-mode configurations. Using standing modes (left), the signal fields and the pump fields are continuously coupled. In systems based on traveling modes (right), the signal fields and the pump fields are periodically coupled in the nonlinear coupling devices, and the coupling time can be controlled, e.g., by the length of the device.

* jqyou@zju.edu.cn

† fnori@riken.jp

approach, we do not require the pump field to be in equilibrium, so the process can potentially be faster. To confirm this, we compare the synchronous pump model with the adiabatic pump model. When the evolution of the pump field is adiabatic, we find that the dynamics is equivalent to the one described by the effective two-photon loss and the two-photon pump. However, when entering the nonequilibrium regime of the pump field, the cat-state generation can acquire higher speed (one order of magnitude larger) and robustness. We also discuss potential implementations of effective synchronous pumps in systems without traveling modes. We show that, by introducing a tunable dissipation to the pump field, an effective synchronous pump can also be realized in standing modes.

Nonequilibrium pump model.—The dissipative generation of cat states is based on the nonlinear coupling between a signal field and a pump field (setting $\hbar = 1$),

$$H_{\text{nl}} = \omega_{\text{pump}} b^\dagger b + \omega_{\text{signal}} a^\dagger a + g_{\text{nl}} [b^\dagger a^2 + b(a^\dagger)^2]. \quad (1)$$

Here, the annihilation operators a and b correspond to a signal mode in the signal field and a pump mode in the pump field, respectively; the frequencies satisfy $\omega_{\text{pump}} = 2\omega_{\text{signal}}$. In the interaction picture, the Hamiltonian can be converted to

$$H_{\text{nl}}^I = g_{\text{nl}} [b^\dagger a^2 + b(a^\dagger)^2]. \quad (2)$$

By introducing a strong loss γ_p and pump terms $[\Omega_p(b + b^\dagger)]$ to the pump field, a master equation for cat-state generation can be obtained in the interaction picture by adiabatically eliminating the pump mode [5, 19–23],

$$\frac{\partial \rho}{\partial t} = -S [[(a^\dagger)^2 - (a)^2], \rho] + \frac{\Gamma_d}{2} \mathcal{L}(a^2, \rho), \quad (3)$$

with the effective two-photon pump intensity $S = 2\Omega_p g_{\text{nl}}/\gamma_p$, the effective two-photon loss rate $\Gamma_d = 4g_{\text{nl}}^2/\gamma_p$, and the Lindblad superoperator $\mathcal{L}(A, \rho) \equiv (2A\rho A^\dagger - A^\dagger A\rho - \rho A^\dagger A)$. This method has successfully been applied to the experimental generation of cat states [28, 29] in superconducting circuits. The speed of the cat-state generation is approximately proportional to Γ_d [27], so that a larger two-photon loss is desirable to obtain increased robustness against signal-field single-photon loss and longer manipulation times for cat states. However, an important condition for Eq. (3) to be valid is $\gamma_p \gg g_{\text{nl}}$, which limits the achievable values of Γ_d . The effective two-photon loss rate Γ_d can be increased by the nonlinear coupling strength g_{nl} , but g_{nl} is usually an intrinsic parameter of the experimental setup used.

While synchronous pumping [30–36] too is based on the nonlinear coupling in Eq. (1), the total system undergoes periodic dynamics with period T_{cycle} , as illustrated in Fig. 1. In each cycle, every time-multiplexed pump mode in the pump field is prepared in a coherent state $|\alpha_p\rangle$ and nonlinearly coupled to the corresponding time-multiplexed signal mode in the signal field. After a period of time t_{nl} , the pump modes are decoupled from the signal modes and reset to vacuum. If there are no

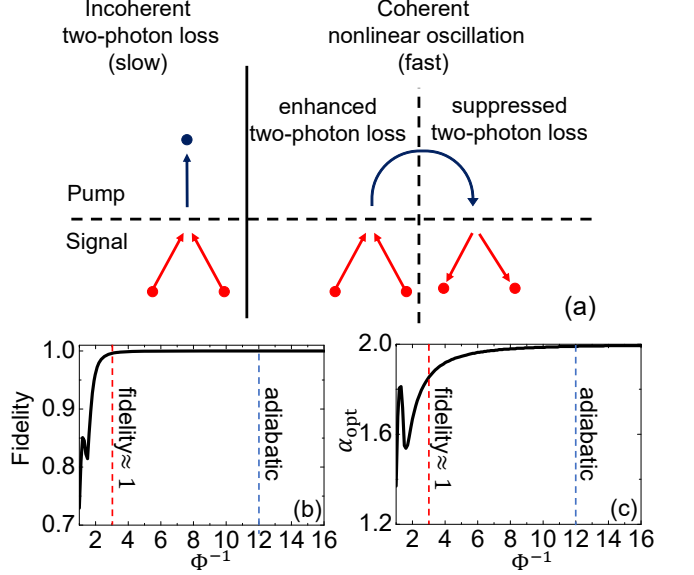


FIG. 2. Cat-state generation based on synchronous pumping (4). (a) Illustration of the two-photon process in an adiabatic pump field and the one in a nonequilibrium pump field, respectively. (b) The highest fidelity with cat states achieved during the discrete evolution with $[\alpha_p \Phi^{-1} = -2i]$. (c) The optimal cat-state size α_{opt} corresponding to the highest fidelity with $[\alpha_p \Phi^{-1} = -2i]$. The coherence between the signal field and the pump field can result in a stronger two-photon loss compared to the adiabatic case, while a very long coupling time, e.g., a vanishing Φ^{-1} , can cause detrimental effects. We find that synchronous pumping (4) can generate nearly perfect cat states for $\Phi^{-1} > 3$, while it approaches the adiabatic model (3) and (5) for $\Phi^{-1} > 12$.

additional operations, e.g., feedback control or coupling between different signal modes, on the signal field, the total system enters a new cycle after some free evolution. The discrete dynamics of a single signal mode can then be modeled as:

$$\rho_{n+1} = \text{Tr}_b \left\{ e^{-iH_{\text{nl}}^I t_{\text{nl}}} \rho_n \otimes |\alpha_p\rangle \langle \alpha_p| e^{iH_{\text{nl}}^I t_{\text{nl}}} \right\}. \quad (4)$$

Here, ρ_n describes the reduced density matrix of the signal mode after n cycles of evolution. The effective pumping intensity per cycle can be controlled by the amplitude of the pump mode α_p and the coupling time t_{nl} . In general, oscillations can occur within each cycle of the coupling (4) due to the coherence between the pump modes and the signal modes as illustrated in Fig. 2(a). Such oscillations can prevent the generation of cat states in continuously coupled standing modes, so that strong losses in the pump fields are necessary to suppress these oscillations. However, the coupling time t_{nl} between traveling modes can be controlled to obtain a maximum flow from the signal field to the pump field, so as to turn an oscillation into a strong two-photon loss.

Note that, with a strong loss in the pump field, the dynamics (4) reduces to Eq. (3) within each cycle. Alternatively, when the amplitude of the pump mode

is small, ($\alpha_p \ll 1$), and the nonlinear evolution time is short, ($g_{nl}t_{nl} \ll 1$), the effective equation of the discrete dynamics (4) without loss is also equivalent to the adiabatic model (3), characterized by the parameter correspondence,

$$S \leftrightarrow \frac{ig_{nl}t_{nl}\alpha_p}{T_{cycle}}, \quad \Gamma_d \leftrightarrow \frac{(g_{nl}t_{nl})^2}{T_{cycle}}. \quad (5)$$

Since the cycle period is always larger than the nonlinear coupling time, $T_{cycle} \geq t_{nl}$, a small $T_{cycle} \approx g_{nl}$ and a large t_{nl} are favored to obtain a large Γ_d . However, when t_{nl} is too large, e.g., $g_{nl}t_{nl} \sim 1$, the discrete evolution (4) can no longer be matched with the perturbative model (3) and (5).

To better understand a pump field out of equilibrium, we consider the condition for cat-state generation based on the synchronous pumping model (4). The steady state of the adiabatic model [Eq. (3)] is a cat state

$$|\text{cat}(\alpha)\rangle \equiv \frac{1}{\sqrt{2+\varepsilon}}(|\alpha\rangle + |-\alpha\rangle), \quad (6)$$

with the complex amplitude $\alpha = i\sqrt{2S/\Gamma_d}$, where $\varepsilon \ll 1$ is a correction to the normalization factor. We now show that the model described by Eq. (4) can generate cat states without resorting to the adiabatic condition, i.e., with a pump field out of equilibrium. The nonlinear evolution time is expressed by the phase term $\Phi = t_{nl}g_{nl}$. To compare with the adiabatic model, we keep $[\alpha_p\Phi^{-1} = -2i]$ constant. By doing so, the steady state in the adiabatic limit is a cat state [Eq. (6)] with the size $\alpha = \sqrt{2i\alpha_p\Phi^{-1}} = 2 \equiv \alpha_{\text{adiab}}$ according to Eqs. (3) and (5). The initial state is assumed to be the vacuum state, and the pumping process is repeated for ($N \approx 30|\Phi^{-1}|$) cycles. After each cycle, we calculate the system fidelity with different cat states $F_{n,\alpha} = \langle \text{cat}(\alpha) | \rho_n | \text{cat}(\alpha) \rangle$. The maximum value of $F_{n,\alpha}$ and the corresponding size α_{opt} are used to characterize the cat-state-generation capacity of the system. We show the relation between Φ^{-1} and the cat-state-generation capacity in Figs. 2(b, c). As cat states with vanishing size, e.g. $\alpha = 0.1$, exhibit few quantum properties, we set the minimum size to be $\alpha = 1.2$.

Figure 2(b) shows that high-fidelity (> 0.9) cat states can be generated for $\Phi^{-1} > 2$. When Φ^{-1} is larger than 12, the generated cat states are close to the prediction of the adiabatic model. For smaller Φ^{-1} , the pump field is no longer in equilibrium, as indicated by the optimal size α_{opt} increasingly deviating from the adiabatic value α_{adiab} . However, the highest fidelity achieved does not decrease significantly in this nonequilibrium regime if Φ^{-1} is larger than 3. There are oscillations for small Φ^{-1} in Figs. 2(b, c), which corresponds to the oscillation illustrated in Fig. 2(a). Therefore, we conclude that the adiabatic condition is unnecessary for cat-state generation under synchronous pumping. Cat states can be generated for $\Phi^{-1} \sim 1$, a regime which cannot be treated perturbatively.

Advantages of nonequilibrium pumping.—As the cat-state generation based on synchronous pumping does not require an adiabatic pump field, one can expect a speed gain. For example, the pump-field loss in experiments is about $\gamma_p \approx 60g_{nl}$ [28]. If the synchronous pump with $\Phi^{-1} = 2$ is applied to a system with the same g_{nl} , the effective Γ_d can be about seven times larger according to Eqs. (3, 5). To confirm this, we calculate the evolution of the optimal fidelity and the optimal size using different pumping schemes, shown in Fig. 3. Without loss of generality, we assume that the discrete evolution (4) contains only the nonlinear coupling part, i.e., $T_{cycle} = t_{nl}$.

In Fig. 3(a), the cat-state fidelity of the discrete dynamics (4) with $\Phi^{-1} = 2$ (black hollow squares) can reach 0.9 after one cycle or at $g_{nl}t = 0.5$, while the adiabatic method Eq. (3) (light green squares) reaches the same fidelity at $g_{nl}t = 4$. For a typical nonlinear coupling strength $g_{nl} = 700$ kHz [28], these two times correspond to about 0.7 μ s and 6 μ s, respectively. However, neither method generates a steady cat state at these times according to α_{opt} in Fig. 3(b). At $g_{nl}t = 3$, the synchronous pumping method obtains the steady fidelity, while the same fidelity appears at $g_{nl}t = 15$ in the adiabatic method. The cost of this speedup is a slight reduction of the steady-state fidelity and cat-state size. To avoid such reduction, a larger Φ^{-1} (red hollow triangles) can be applied, with which a moderate speedup can still be obtained almost without any cost. As the generation of large cat states is faster [27], we consider an adiabatic model with a weak pump $S = -1.4\Gamma_d$ (violet triangles), which results in the cat-state size of the discrete dynamics with $\Phi^{-1} = 2$. Indeed, in Fig. 3(b), the asymptotic optimal size α_{opt} of the weakly pumped adiabatic model (violet triangles) nearly coincides with the one of the discrete dynamics with $\Phi^{-1} = 2$ (black hollow squares). The fidelity of the weakly pumped adiabatic model (violet triangles) first reaches 0.9 at $g_{nl}t = 5$, which is one order of magnitude larger than the time for the discrete dynamics with $\Phi^{-1} = 2$ (black hollow squares) to reach the same fidelity. In addition to the transient states, the time for the adiabatic model with $S = -1.4\Gamma_d$ (violet triangles) to approach the steady state is also one order of magnitude larger compared to the discrete dynamics with $\Phi^{-1} = 2$ (black hollow squares).

Note that there are oscillations in the curves in Fig. 3(a), which may be due to the existence of a truncation value of α_{opt} . These oscillations happen at times with α_{opt} exceeding the minimum value. Another concern may be whether these short-time states with minimum size $\alpha_{\text{opt}} = 1.2$ in Figs. 3(a, b) are cat states or not. Therefore, we plot the Wigner function after the first cycle of the discrete dynamics (4) with $\Phi^{-1} = 2$ (the first black hollow square) in Fig. 3(c), which shows evidence of a cat-like state. Compared to the steady Wigner function at $t = 4/g_{nl}$ in Fig. 3(d) (the eighth black hollow square in Fig. 3(a)), the two components at $|\pm \alpha_{\text{opt}}\rangle$ appear

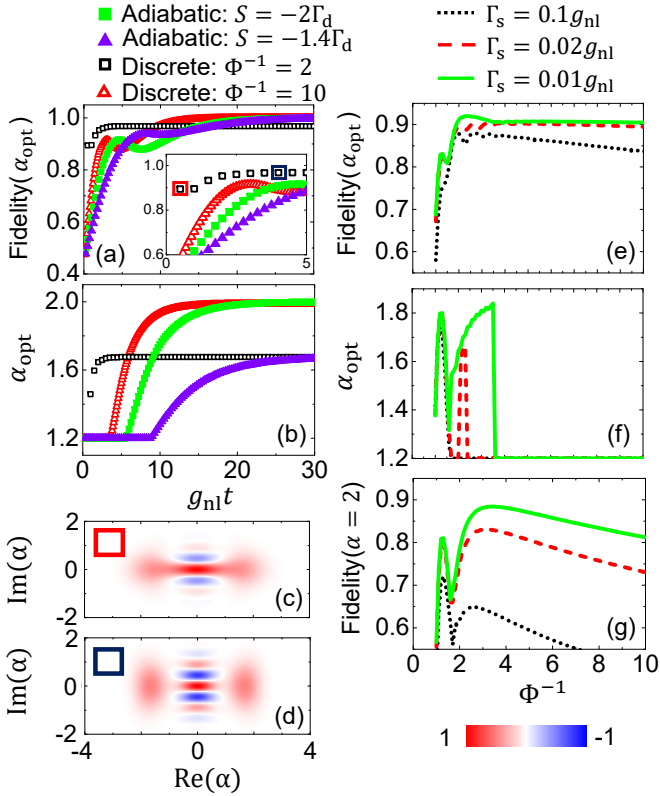


FIG. 3. (a)-(d) Comparison between the discrete evolution (4) and the adiabatic model (3). The effective two-photon loss rate for the adiabatic model is $\Gamma_d = 0.064g_{\text{nl}}$; the parameter for the synchronous pumping is $\alpha_p\Phi^{-1} = -2i$. (a) The highest fidelity with optimized cat states at different times. Results for $g_{\text{nl}}t < 5$ are shown in the inset. (b) The optimal cat-state size corresponding to the highest fidelity in (a). (c,d) Wigner functions of the discrete evolution with $\Phi^{-1} = 2$ (black hollow squares in (a,b)) at $t = 0.5/g_{\text{nl}}$ and $t = 4/g_{\text{nl}}$, respectively. The synchronous pumping in the nonequilibrium regime is found to be one order of magnitude faster compared to the adiabatic method used in experiments [28]. (e)-(g) Synchronous pumping in the presence of the single-photon loss (7). The pump field is set to be $\alpha_p\Phi^{-1} = -2i$. (e) Relation between the highest achievable fidelity and the nonlinear evolution time Φ . (f) The relation between the optimal size α_{opt} corresponding to highest fidelity and the nonlinear evolution time Φ . (g) The highest fidelity according to the cat state with $\alpha = 2$. Optimal values of Φ^{-1} are always far away from the adiabatic limit, $(\Phi^{-1} > 12)$. We find that the synchronous pumping model with a nonequilibrium pump field exhibits higher speed and robustness against single-photon loss compared to the methods with adiabatic pump fields.

squeezed, and the interference pattern is faint.

In optical systems [30–36], the main challenge for cat-state generation is the strong detrimental single-photon loss [43]. Although synchronous pumping is commonly used in nonlinear optics, the adiabatic model remains valid in many cases due to the strong single-photon loss. However, operating nonlinear optical systems in

the quantum regime is necessary for applications in quantum information [6]. Therefore, we now analyze the performance of the nonequilibrium pump field in the presence of single-photon loss. To describe the latter, we can introduce loss terms in Eq. (4) as follows:

$$\dot{\rho}_n(t) = -i[H_{\text{nl}}^{\text{I}}, \rho_n(t)] + \frac{\Gamma_s}{2}\mathcal{L}(a, \rho_n(t)) + \frac{\Gamma_s}{2}\mathcal{L}(b, \rho_n(t)), \quad \rho_n(0) = \rho_n \otimes |\alpha_p\rangle\langle\alpha_p|, \quad \rho_{n+1} = \text{Tr}_b\{\rho_n(t_{\text{nl}})\}. \quad (7)$$

Here, we assume that the signal mode a and the pump mode b have the same single-photon loss rate Γ_s .

In Figs. 3(e, f), we show the fidelity with optimized cat states and the corresponding optimal sizes α_{opt} , which are calculated in the same way as in Fig. 2. When Φ^{-1} is larger than 5, the accessible fidelity decreases with increasing Φ^{-1} . In this regime, the optimal size α_{opt} always drops below the minimum value indicating a transient cat state [Fig. 3(c)]. These transient states can be reached in a short time, avoiding the influence of single-photon loss. The optimal value of Φ^{-1} in Fig. 3(e) ranges from 3 to 2, which is far below the adiabatic limit, $\Phi^{-1} > 12$, indicated in Fig. 2. The sudden drops in Fig. 3(f) correspond to the competition between the transient cat state in Fig. 3(c) and the steady cat state in Fig. 3(d). The steady cat state has higher fidelity in ideal cases, but the transient one is less influenced by the single-photon loss. In some cases, the objective may be to create cat states with certain target sizes. Therefore, we also calculate the fidelity with a cat state of ideal adiabatic size $\alpha = 2$, as shown in Fig. 3(g). We find that, due to the fixed size, the qualities of cat states are reduced compared to the ones in Fig. 3(f). In addition, the highest accessible fidelity is more sensitive to the choice of Φ^{-1} .

Hence, we find that entering the nonequilibrium regime of the synchronous pumping can significantly increase the speed and the robustness of cat-state generation. Compared to current methods of cat-state generation, the speed of the synchronous pumping method can be one order of magnitude larger. By choosing an optimized nonlinear interaction time t_{nl} , which is far away from the adiabatic limit $\Phi^{-1} > 12$, the qualities of cat states can be more distinct in the presence of single-photon-signal-mode loss.

Applying synchronous pumping in standing modes.— To utilize a nonequilibrium pump field for cat-state generation, the synchronous pumping method is necessary. While the synchronous pumping is widely used in optical systems based on traveling modes, it is not obvious how to apply this method to standing modes, as they occur, e.g., in superconducting resonators. In traveling modes, the pump mode can be separated from the signal mode and reset, because the pump mode and the signal mode have different group velocities. However, standing modes have vanishing group velocities. Therefore, an additional mechanism is required to reset the pump mode. This can be achieved by a switchable loss channel coupled to the pump mode. During the nonlinear coupling,

this channel is off, so that the dynamics is governed by the Hamiltonian in Eq. (2). At the end of each cycle of evolution described by Eq. (4), we then turn on a strong loss channel to evacuate the pump mode. After the depletion, the pump mode can be prepared in a coherent state by a strong pump. Such a loss channel can be realized by widely used setups in superconducting circuits [44–56], in which the cavity frequencies or the coupling strengths can be adjusted. By coupling a lossy superconducting resonator to the pump field, a loss can be introduced. Such a loss can be shut down by detuning the lossy cavity from the pump mode or by reducing the coupling strength. With currently accessible parameters, the loss rate can be changed between $0.01g_{\text{nl}}$ and $10g_{\text{nl}}$ [44–56].

Conclusions.—We considered dissipative cat-state generation with a synchronous pump field in the nonequilibrium regime. A nonequilibrium pump field, which cannot be adiabatically eliminated, was shown to be capable of generating high-quality cat states. Our numerical results confirm that cat-state generation can be enhanced in the nonequilibrium regime. Compared to the adiabatic method, the speed of generation can be increased by more than one order of magnitude, and the fidelity is less affected by the single-photon loss. These benefits result from faster two-photon processes, made possible by abandoning the requirement of adiabatic pump fields. We also discussed the application of

synchronous pumping in systems based on standing modes. Synchronous pumping can then be realized by well-developed setups in superconducting circuits, which are commonly used platforms for cat-state generation. Therefore, our work provides a method to improve the cat-state generation in different systems, and reveals that synchronously pumped systems may be advantageous for generating cat states.

J.Q.Y. is partially supported by the National Natural Science Foundation of China (NSFC) (Grant No. 11774022 and No. U1801661) and the National Key Research and Development Program of China (Grant No. 2016YFA0301200). F.N. is supported in part by: Nippon Telegraph and Telephone Corporation (NTT) Research, the Japan Science and Technology Agency (JST) [via the Quantum Leap Flagship Program (Q-LEAP), the Moonshot R&D Grant Number JPMJMS2061, and the Centers of Research Excellence in Science and Technology (CREST) Grant No. JPMJCR1676], the Japan Society for the Promotion of Science (JSPS) [via the Grants-in-Aid for Scientific Research (KAKENHI) Grant No. JP20H00134 and the JSPS-CRFBR Grant No. JPJSBP120194828], the Army Research Office (ARO) (Grant No. W911NF-18-1-0358), the Asian Office of Aerospace Research and Development (AOARD) (via Grant No. FA2386-20-1-4069), and the Foundational Questions Institute Fund (FQXi) via Grant No. FQXi-IAF19-06.

- [1] C. Monroe, D. M. Meekhof, B. E. King, and D. J. Wineland, “A ‘Schrödinger cat’ superposition state of an atom,” *Science* **272**, 1131–1136 (1996).
- [2] D. Leibfried, E. Knill, S. Seidelin, J. Britton, R. B. Blakestad, J. Chiaverini, D. B. Hume, W. M. Itano, J. D. Jost, C. Langer, R. Ozeri, R. Reichle, and D. J. Wineland, “Creation of a six-atom ‘Schrödinger cat’ state,” *Nature* **438**, 639–642 (2005).
- [3] Samuel Deléglise, Igor Dotsenko, Clément Sayrin, Julien Bernu, Michel Brune, Jean-Michel Raimond, and Serge Haroche, “Reconstruction of non-classical cavity field states with snapshots of their decoherence,” *Nature* **455**, 510–514 (2008).
- [4] Brian Vlastakis, Gerhard Kirchmair, Zaki Leghtas, Simon E. Nigg, Luigi Frunzio, S. M. Girvin, Mazyar Mirrahimi, M. H. Devoret, and R. J. Schoelkopf, “Deterministically encoding quantum information using 100-photon Schrödinger cat states,” *Science* **342**, 607–610 (2013).
- [5] Mark J. Everitt, Timothy P. Spiller, Gerard J. Milburn, Richard D. Wilson, and Alexandre M. Zagoskin, “Engineering dissipative channels for realizing schr/”odinger cats in SQUIDs,” *Frontiers in ICT* **1**, 1 (2014).
- [6] Yoshihisa Yamamoto, Kazuyuki Aihara, Timothee Leleu, Ken-ichi Kawarabayashi, Satoshi Kako, Martin Fejer, Kyo Inoue, and Hiroki Takesue, “Coherent Ising machines-optical neural networks operating at the quantum limit,” *npj Quantum Information* **3**, 49 (2017).
- [7] Zhaoyou Wang, Marek Pechal, E. Alex Wollack, Patricio Arrangoiz-Arriola, Maodong Gao, Nathan R. Lee, and Amir H. Safavi-Naeini, “Quantum dynamics of a few-photon parametric oscillator,” *Phys. Rev. X* **9**, 021049 (2019).
- [8] D. Leibfried, M. D. Barrett, T. Schaetz, J. Britton, J. Chiaverini, W. M. Itano, J. D. Jost, C. Langer, and D. J. Wineland, “Toward Heisenberg-limited spectroscopy with multiparticle entangled states,” *Science* **304**, 1476–1478 (2004).
- [9] Tomohisa Nagata, Ryo Okamoto, Jeremy L. O’Brien, Keiji Sasaki, and Shigeki Takeuchi, “Beating the standard quantum limit with four-entangled photons,” *Science* **316**, 726–729 (2007).
- [10] Jonathan A. Jones, Steven D. Karlen, Joseph Fitzsimons, Arzhang Ardavan, Simon C. Benjamin, G. Andrew D. Briggs, and John J. L. Morton, “Magnetic field sensing beyond the standard quantum limit using 10-spin N00N states,” *Science* **324**, 1166–1168 (2009).
- [11] M. Kira, S. W. Koch, R. P. Smith, A. E. Hunter, and S. T. Cundiff, “Quantum spectroscopy with Schrödinger-cat states,” *Nature Physics* **7**, 799–804 (2011).
- [12] Adrien Facon, Eva-Katharina Dietsche, Dorian Gross, Serge Haroche, Jean-Michel Raimond, Michel Brune, and Sébastien Gleyzes, “A sensitive electrometer based on a Rydberg atom in a Schrödinger-cat state,” *Nature* **535**, 262–265 (2016).
- [13] T. Choi, S. Debnath, T. A. Manning, C. Figgatt, Z.-X.

Gong, L.-M. Duan, and C. Monroe, "Optimal quantum control of multimode couplings between trapped ion qubits for scalable entanglement," *Phys. Rev. Lett.* **112**, 190502 (2014).

[14] Reinier W. Heeres, Philip Reinhold, Nissim Ofek, Luigi Frunzio, Liang Jiang, Michel H. Devoret, and Robert J. Schoelkopf, "Implementing a universal gate set on a logical qubit encoded in an oscillator," *Nature Communications* **8**, 94 (2017).

[15] L. Hu, Y. Ma, W. Cai, X. Mu, Y. Xu, W. Wang, Y. Wu, H. Wang, Y. P. Song, C.-L. Zou, S. M. Girvin, L.-M. Duan, and L. Sun, "Quantum error correction and universal gate set operation on a binomial bosonic logical qubit," *Nature Physics* **15**, 503–508 (2019).

[16] Chuan-Sheng Yang, Yan-Lei Zhang, Guang-Can Guo, and Xu-Bo Zou, "Experimentally feasible scheme for a high-fidelity controlled-phase gate with general cat-state qubits," *Phys. Rev. A* **100**, 062324 (2019).

[17] Jérémie Guillaud and Mazyar Mirrahimi, "Repetition cat qubits for fault-tolerant quantum computation," *Phys. Rev. X* **9**, 041053 (2019).

[18] Xiao-Ling He, Zhen-Fei Zheng, Yu Zhang, and Chui-Ping Yang, "One-step transfer of quantum information for a photonic cat-state qubit," *Quantum Information Processing* **19**, 80 (2020).

[19] L. Gilles and P. L. Knight, "Two-photon absorption and nonclassical states of light," *Phys. Rev. A* **48**, 1582–1593 (1993).

[20] L. Gilles, B. M. Garraway, and P. L. Knight, "Generation of nonclassical light by dissipative two-photon processes," *Phys. Rev. A* **49**, 2785–2799 (1994).

[21] E. S. Guerra, B. M. Garraway, and P. L. Knight, "Two-photon parametric pumping versus two-photon absorption: A quantum jump approach," *Phys. Rev. A* **55**, 3842–3857 (1997).

[22] Huatang Tan, F. Bariani, Gaoxiang Li, and P. Meystre, "Generation of macroscopic quantum superpositions of optomechanical oscillators by dissipation," *Phys. Rev. A* **88**, 023817 (2013).

[23] Xin Wang, Adam Miranowicz, Hong-Rong Li, and Franco Nori, "Hybrid quantum device with a carbon nanotube and a flux qubit for dissipative quantum engineering," *Phys. Rev. B* **95**, 205415 (2017).

[24] S. Ashhab and Franco Nori, "Qubit-oscillator systems in the ultrastrong-coupling regime and their potential for preparing nonclassical states," *Phys. Rev. A* **81**, 042311 (2010).

[25] R. Y. Teh, P. D. Drummond, and M. D. Reid, "Overcoming decoherence of Schrödinger cat states formed in a cavity using squeezed-state inputs," *Phys. Rev. Research* **2**, 043387 (2020).

[26] Ye-Hong Chen, Wei Qin, Xin Wang, Adam Miranowicz, and Franco Nori, "Shortcuts to adiabaticity for the quantum Rabi model: Efficient generation of giant entangled cat states via parametric amplification," *Phys. Rev. Lett.* **126**, 023602 (2021).

[27] Wei Qin, Adam Miranowicz, Hui Jing, and Franco Nori, "Generating long-lived macroscopically distinct superposition states in atomic ensembles," *Phys. Rev. Lett.* **127**, 093602 (2021).

[28] Z. Leghtas, S. Touzard, I. M. Pop, A. Kou, B. Vlastakis, A. Petrenko, K. M. Sliwa, A. Narla, S. Shankar, M. J. Hatridge, M. Reagor, L. Frunzio, R. J. Schoelkopf, M. Mirrahimi, and M. H. Devoret, "Confining the state of light to a quantum manifold by engineered two-photon loss," *Science* **347**, 853–857 (2015).

[29] S. Touzard, A. Grimm, Z. Leghtas, S. O. Mundhada, P. Reinhold, C. Axline, M. Reagor, K. Chou, J. Blumoff, K. M. Sliwa, S. Shankar, L. Frunzio, R. J. Schoelkopf, M. Mirrahimi, and M. H. Devoret, "Coherent oscillations inside a quantum manifold stabilized by dissipation," *Phys. Rev. X* **8**, 021005 (2018).

[30] M. G. Raymer, P. D. Drummond, and S. J. Carter, "Limits to wideband pulsed squeezing in a traveling-wave parametric amplifier with group-velocity dispersion," *Opt. Lett.* **16**, 1189–1191 (1991).

[31] G. Patera, N. Treps, C. Fabre, and G. J. de Valcárcel, "Quantum theory of synchronously pumped type I optical parametric oscillators: characterization of the squeezed supermodes," *The European Physical Journal D* **56**, 123 (2009).

[32] C. Y. Jiang, J. S. Liu, B. Sun, K. J. Wang, S. X. Li, and J. Q. Yao, "Time-dependent theoretical model for terahertz wave detector using a parametric process," *Opt. Express* **18**, 18180–18189 (2010).

[33] V. A. Averchenko, Yu. M. Golubev, C. Fabre, and N. Treps, "Quantum correlations and fluctuations in the pulsed light produced by a synchronously pumped optical parametric oscillator below its oscillation threshold," *The European Physical Journal D* **61**, 207 (2011).

[34] Ryan Hamerly, Alireza Marandi, Marc Jankowski, M. M. Fejer, Yoshihisa Yamamoto, and Hideo Mabuchi, "Reduced models and design principles for half-harmonic generation in synchronously pumped optical parametric oscillators," *Phys. Rev. A* **94**, 063809 (2016).

[35] Marc Jankowski, Alireza Marandi, C. R. Phillips, Ryan Hamerly, Kirk A. Ingold, Robert L. Byer, and M. M. Fejer, "Temporal multistates in optical parametric oscillators," *Phys. Rev. Lett.* **120**, 053904 (2018).

[36] Arkadev Roy, Saman Jahani, Carsten Langrock, Martin Fejer, and Alireza Marandi, "Spectral phase transitions in optical parametric oscillators," *Nature Communications* **12**, 835 (2021).

[37] P. Kinsler and P. D. Drummond, "Quantum dynamics of the parametric oscillator," *Phys. Rev. A* **43**, 6194–6208 (1991).

[38] Hua Deng, Daniel Erenso, Reeta Vyas, and Surendra Singh, "Entanglement, interference, and measurement in a degenerate parametric oscillator," *Phys. Rev. Lett.* **86**, 2770–2773 (2001).

[39] Alireza Marandi, Zhe Wang, Kenta Takata, Robert L. Byer, and Yoshihisa Yamamoto, "Network of time-multiplexed optical parametric oscillators as a coherent Ising machine," *Nature Photonics* **8**, 937–942 (2014).

[40] Peter L. McMahon, Alireza Marandi, Yoshitaka Haribara, Ryan Hamerly, Carsten Langrock, Shuhei Tamate, Takahiro Inagaki, Hiroki Takesue, Shoko Utsunomiya, Kazuyuki Aihara, Robert L. Byer, M. M. Fejer, Hideo Mabuchi, and Yoshihisa Yamamoto, "A fully programmable 100-spin coherent Ising machine with all-to-all connections," *Science* **354**, 614–617 (2016).

[41] Takahiro Inagaki, Yoshitaka Haribara, Koji Igarashi, Tomohiro Sonobe, Shuhei Tamate, Toshimori Honjo, Alireza Marandi, Peter L. McMahon, Takeshi Umeiki, Koji Enbusu, Osamu Tadanaga, Hirokazu Takenouchi, Kazuyuki Aihara, Kenichi Kawarabayashi, Kyo Inoue, Shoko Utsunomiya, and Hiroki Takesue, "A coherent Ising machine for 2000-node optimization problems,"

Science **354**, 603–606 (2016).

[42] Atsushi Yamamura, Kazuyuki Aihara, and Yoshihisa Yamamoto, “Quantum model for coherent Ising machines: Discrete-time measurement feedback formulation,” *Phys. Rev. A* **96**, 053834 (2017).

[43] Zheng-Yang Zhou, Clemens Gneiting, J. Q. You, and Franco Nori, “Generating and detecting entangled cat states in dissipatively coupled degenerate optical parametric oscillators,” *Phys. Rev. A* **104**, 013715 (2021).

[44] A. Palacios-Laloy, F. Nguyen, F. Mallet, P. Bertet, D. Vion, and D. Esteve, “Tunable resonators for quantum circuits,” *Journal of Low Temperature Physics* **151**, 1034 (2008).

[45] M. Sandberg, C. M. Wilson, F. Persson, T. Bauch, G. Johansson, V. Shumeiko, T. Duty, and P. Delsing, “Tuning the field in a microwave resonator faster than the photon lifetime,” *Applied Physics Letters* **92**, 203501 (2008).

[46] Y. Kubo, F. R. Ong, P. Bertet, D. Vion, V. Jacques, D. Zheng, A. Dréau, J.-F. Roch, A. Auffeves, F. Jelezko, J. Wrachtrup, M. F. Barthe, P. Bergonzo, and D. Esteve, “Strong coupling of a spin ensemble to a superconducting resonator,” *Phys. Rev. Lett.* **105**, 140502 (2010).

[47] M. Pechal, J.-C. Besse, M. Mondal, M. Oppliger, S. Gasparinetti, and A. Wallraff, “Superconducting switch for fast on-chip routing of quantum microwave fields,” *Phys. Rev. Applied* **6**, 024009 (2016).

[48] Wei Qin, Ye-Hong Chen, Xin Wang, Adam Miranowicz, and Franco Nori, “Strong spin squeezing induced by weak squeezing of light inside a cavity,” *Nanophotonics* **9**, 4853–4868 (2020).

[49] Sumedh Mahashabde, Ernst Otto, Domenico Montemurro, Sebastian de Graaf, Sergey Kubatkin, and Andrey Danilov, “Fast tunable high- Q -factor superconducting microwave resonators,” *Phys. Rev. Applied* **14**, 044040 (2020).

[50] P. Bertet, C. J. P. M. Harmans, and J. E. Mooij, “Parametric coupling for superconducting qubits,” *Phys. Rev. B* **73**, 064512 (2006).

[51] Matteo Mariantoni, Frank Deppe, A. Marx, R. Gross, F. K. Wilhelm, and E. Solano, “Two-resonator circuit quantum electrodynamics: A superconducting quantum switch,” *Phys. Rev. B* **78**, 104508 (2008).

[52] Matteo Mariantoni, H. Wang, Radoslaw C. Bialczak, M. Lenander, Erik Lucero, M. Neeley, A. D. O’Connell, D. Sank, M. Weides, J. Wenner, T. Yamamoto, Y. Yin, J. Zhao, John M. Martinis, and A. N. Cleland, “Photon shell game in three-resonator circuit quantum electrodynamics,” *Nature Physics* **7**, 287 (2011).

[53] A. Baust, E. Hoffmann, M. Haeberlein, M. J. Schwarz, P. Eder, J. Goetz, F. Wulschner, E. Xie, L. Zhong, F. Quijandria, B. Peropadre, D. Zueco, J.-J. García Ripoll, E. Solano, K. Fedorov, E. P. Menzel, F. Deppe, A. Marx, and R. Gross, “Tunable and switchable coupling between two superconducting resonators,” *Phys. Rev. B* **91**, 014515 (2015).

[54] Yao Lu, S. Chakram, N. Leung, N. Earnest, R. K. Naik, Ziwen Huang, Peter Groszkowski, Eliot Kapit, Jens Koch, and David I. Schuster, “Universal stabilization of a parametrically coupled qubit,” *Phys. Rev. Lett.* **119**, 150502 (2017).

[55] Qi-Ming Chen, Yu-xi Liu, Luyan Sun, and Re-Bing Wu, “Tuning the coupling between superconducting resonators with collective qubits,” *Phys. Rev. A* **98**, 042328 (2018).

[56] Michele C. Collodo, Anton Potočnik, Simone Gasparinetti, Jean-Claude Besse, Marek Pechal, Mahdi Sameti, Michael J. Hartmann, Andreas Wallraff, and Christopher Eichler, “Observation of the crossover from photon ordering to delocalization in tunably coupled resonators,” *Phys. Rev. Lett.* **122**, 183601 (2019).

[57] Ze-Liang Xiang, Sahel Ashhab, J. Q. You, and Franco Nori, “Hybrid quantum circuits: Superconducting circuits interacting with other quantum systems,” *Rev. Mod. Phys.* **85**, 623–653 (2013).

[58] Raphaël Lescanne, Marius Villiers, Théau Peronnin, Alain Sarlette, Matthieu Delbecq, Benjamin Huard, Takis Kontos, Mazyar Mirrahimi, and Zaki Leghtas, “Exponential suppression of bit-flips in a qubit encoded in an oscillator,” *Nature Physics* **16**, 509–513 (2020).